6092 *Macromolecules* **2010**, *43*, 6092–6098
DOI: 10.1021/ma100918e

Macromolecules
ARTICLE

Dielectric Relaxation Behavior of Polymerized Ionic Liquid

Kenji Nakamura,* Tatsuya Saiwaki, and Koji Fukao

Department of Physical Sciences, Ritsumeikan University, Kusatsu, Shiga 525-8577, Japan

Received April 26, 2010; Revised Manuscript Received June 14, 2010

ABSTRACT: Dynamic aspects of a polymerized ionic liquid, poly(1-ethyl-3-vinylimidazolium bis(trifluoromethanesulfonylimide)), were investigated using a broadband dielectric spectroscopy method in the frequency range of 10 mHz to 2 MHz and temperatures ranging from −90 to +90 °C. The polymerized ionic liquid shows three relaxation modes including the relaxation mode due to the effect of electrode polarization behavior. We attribute the slow relaxation mode to the segmental motion of the polymer main chain and the fast mode to the rotational motion of the polymer side chain. Relaxation times of these relaxation modes and the specific direct current conductivity showed an Arrhenius-type temperature dependence at temperatures above and below the glass transition temperature of the polymer. In order to explain the less fragile property of the polymerized ionic liquid, we propose that the ion transport mechanism is achieved by the formation and dissociation of ion-pairs formed between a positively charged 1-ethyl-3-vinylimidazolium monomer unit in a polymer chain and a negatively charged bis(trifluoromethanesulfonylimide).

Introduction

Ionic liquids (ILs) are organic molten salts consisting of a pair of soft cationic and anionic species. They display unique properties such as nonvolatility, nonflammability and high electric conductivity.[1−3] Many scientists and engineers have studied ILs for use as media in chemical reactions[2,4] or constituent materials for optical/electronic devices.[5] Recently, physicochemical studies of ILs have also been much investigated.[6,7]

Ohno and his co-worker were the first to synthesize polymerized ionic liquids (PILs) made from IL monomers.[8] Since PILs are not liquid but solid, they lose the special characteristics of liquids. For example, PILs have lower conductivity than low-molecular weight ILs due to a large increase in bulk viscosity.[8] However, PILs retain such special properties as the nonflammability or stability of ILs and have higher conductivity than electrically neutral polymers like polystyrene. Since solid state polymer materials are easily downsized and molded to make products, PILs have also received much research interest for their potential applications.[9,10] At the present time, there are reports about the synthesis and characterization of PILs[11−13] and a few reports about the physicochemical properties of PILs.[14,15]

PILs can be classified as one of the polyelectrolyte species—typified by sodium polystyrenesulfonate or poly(acrylic acid)—in the sense that they consist of an electrolyte monomer unit. Since most polyelectrolytes are soluble in water and dissociate into a charged polyelectrolyte chain and oppositely charged counterions, physicochemical properties of polyelectrolytes in water media have been the main focus of studies.[16,17] On the other hand, physicochemical features of linear polyelectroltyes in the solid state have been less thoroughly investigated due to their hygroscopic nature.[16]

It is well-known that ILs bearing hydrophobic counterions like PF_6^- are insoluble in water.[2,3] PILs also become water-insoluble if hydrophobic ions are chosen as a counterion at the synthetic stage. In contrast, PILs are soluble in polar organic solvents and transparent films can be made by solution casting; as is the case for ordinary polymer casting.[18] These properties of PILs led us to speculate that PILs can be regarded as model substances of solid state polyelectrolytes to study the bulk nature of polyelectrolyte systems. In the first step of this project, we focused on the kinetics of bulk PILs by investigating the dielectric relaxation (DR) behavior of poly(1-ethyl-3-vinylimidazolium bis(trifluoromethanesulfonylimide)) ($PC_2VITFSI$) (Figure 1), which is a typical PIL species and water-insoluble because its counteranion, bis(trifluoromethanesulfonylimide) ($TFSI^-$), is hydrophobic.[8,10,18]

DR techniques are powerful tools to investigate the motion of molecules or substituent groups over a broad time range, on the order of $10^{-11}-10^{2}$ s. If the molecules or substituent groups bear electric dipole moments, then DR provides useful information on the sizes of dipoles and the time scale of their molecular motions. Therefore, DR measurements have been widely employed for the study of either polymer or low molecular weight systems.[19−21] In polymer systems, the relaxation modes concerning their dynamics, e.g. segmental or side chain motions, were observed in the frequency range on the orders of mHz to MHz. On the other hand, low molecular weight substances (liquid state); whose molecular motions are faster than that of macromolecular system, exhibit relaxation modes around the frequency region on the orders of MHz to GHz.

Some DR studies on ILs have previously been reported.[22−24] According to these studies the main relaxation modes observed in IL system were related to the rotational motion of ions or ion-pairs formed between a cation and an anion in the IL molecules. Alternately, there are few studies for DR[25] or impedance behavior[26] of PILs. Shen has studied the DR behavior of the PIL series of poly(1-(*p*-vinylbenzyl)-3-butylimidazolum) with various counteranions in the frequency ranged from 50 MHz to 10 GHz.[25] They focused on the dielectric constants of PILs and ion-pair motions. As mentioned above, it is difficult to observe macro dynamics of polymers in this frequency range. Impedance analysis studied by Ohno focused on the transport properties of Li^+ ions in a neat PIL or cross-linked PIL matrix and focused less on the dynamics of PILs.[26] Our DR measurement frequency ranged from 10 mHz to 2 MHz corresponded to the time scale of macro dynamics of polymers. In order to discuss the essential dynamics

*To whom correspondence should be addressed. E-mail: kenjin@se.ritsumei.ac.jp.

 Published on Web 06/22/2010

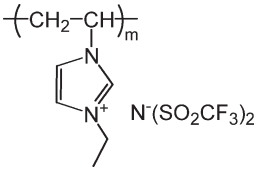

Figure 1. Chemical structure of poly(1-ethyl-3-vinylimidazolium bis(trifluoromethanesulfonylimide)) ($PC_2VITFSI$).

of PILs; we compared DR behavior and dynamics of PILs with those observed in ILs[22−24] or ionomer polymers,[27−29] which possess a few electrolyte monomer units on the polymer chain backbone.

Experimental Section

Materials. 1-Vinylimidazole was purchased from Tokyo Kasei (Tokyo). Bromoethane and 2,2′-azobis(isobutyronitrile) (AIBN) were purchased from Wako Pure Chemicals (Osaka). Lithium bis(trifluoromethanesulfonyl)imide (LiTFSI) was purchased from Kanto Chemical (Tokyo). DMSO-d_6 and acetone-d_6 were purchased from ISOTEC Inc. (Cambridge) and used as a solvent for NMR measurements. All of the reagents were used without further purification.

Synthesis. 1-Ethyl-3-vinylimidazolium bromide was prepared by refluxing the mixture of 1-vinylimidazole (7.1 g, 75 mmol) and excess bromoethane (12.3 g, 113 mmol) in an ethanol solution (8 mL) at 50 °C for 4 days.[8] After the ethanol and unreacted bromoethane were completely evaporated from the solution, 1-ethyl-3-vinylimidazolium bromide was dried under vacuum at 70 °C (97% yield). 1-Ethyl-3-vinylimidazolium bromide (14.9 g, 73 mmol) was dissolved in aqueous solution (70 mL) with a slight excess of LiTFSI (25.7 g, 90 mmol) and stirred for 4 days at room temperature. The resultant ionic liquid phase of 1-ethyl-3-vinylimidazolium bis(trifluoromethanesulfonyl)imide ($C_2VITFSI$) was separated from the aqueous phase and washed with water five times. After completely evaporating the remaining water, $C_2VITFSI$ was dried under vacuum at 50 °C (88% yield). The purity of $C_2VITFSI$ was confirmed using ^{1}H NMR measurements in DMSO-d_6 (Figure S1 in the Supporting Information).[18] The absence of AgBr precipitation after an addition of aqueous $AgNO_3$ solution indicated that bromide salts were eliminated from the $C_2VITFSI$.

$PC_2VITFSI$ was synthesized via the free radical polymerization of $C_2VITFSI$ (10.1 g, 25 mmol); polymerization was initiated by AIBN (41 mg, 0.25 mmol) in DMSO (35 mL) solution at 60 °C for 16 h. $PC_2VITFSI$ was precipitated by pouring the resultant solution into an excess ethanol solution. Repeating the precipitation from DMSO to ethanol solution purified the crude $PC_2VITFSI$ (67% yield). The purity of $PC_2VITFSI$ was confirmed using ^{1}H NMR measurements in acetone-d_6 (Figure S1 in the Supporting Information).[18]

Measurements. The intrinsic viscosity ($[\eta]$) of $PC_2VITFSI$ was measured using an Ubbelode-type viscometer at 30 °C in methylethylketone (MEK) containing 75 mM LiTFSI and estimated as $[\eta] = 10.95\ cm^3g^{-1}$. The value of the viscosity average molecular weight (M_v) for $PC_2VITFSI$ was estimated as $M_v = 4.2 \times 10^4$ by employing the Mark−Houwink−Sakurada equation, $[\eta] = KM_v^a$, with parameters of $K = 2.3 \times 10^{-2}\ cm^3\ g^{-1}$ and $a = 0.62$. These parameters were determined in the system of polystyrene/MEK solution at 30 °C.[30,31]

^{1}H NMR measurements were performed using a NMR spectrometer (JNM-ECA-400, JEOL, Tokyo, Japan) with a proton resonance frequency of 400 MHz to characterize the synthesized ILs and PILs at 30 °C.

The glass-transition temperature (T_g) of $PC_2VITFSI$ was estimated using a differential scanning calorimeter (DSC) (EXSTAR DSC6000, SII, Chiba, Japan) at a heating and cooling rate of 10 K/min. The measurement temperature range was from −110 to +140 °C. The glass-transition temperature T_g was determined from the midpoint of the total heat flow curve in the thermal transition region.

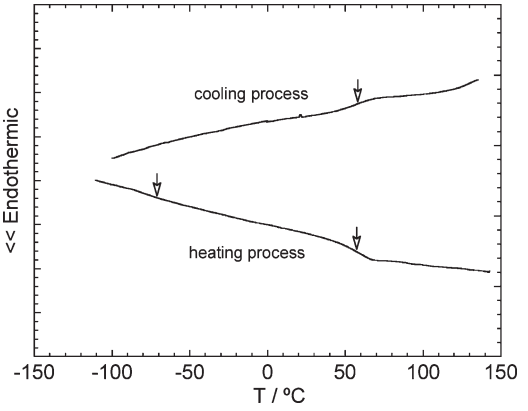

Figure 2. DSC profile of $PC_2VITFSI$. The upper and lower curves represent the total heat flow during the cooling and heating process, respectively. Arrows indicate the temperature showing thermal transition.

Dielectric relaxation measurements were performed using two measuring systems. The LCR meter (E4980A, Agilent, CA, USA) was used for the angular frequency (ω) range from 1.36×10^2 to 1.36×10^7 rad s^{-1}. The impedance analyzer, (SI1260, Solartron Instruments, Hampshire, U.K.) including the dielectric measurement interface (SI1296, Solartron Instruments, Hampshire, U.K.), was used for the ω range from 6.28×10^{-2} to 6.28×10^6 rad s^{-1}. The obtained real and imaginary part of electric capacitance (C' and C'') were converted to the real and imaginary part of the relative electric permittivity (ε' and ε'') using the relationships $\varepsilon' = C'C_0^{-1}$ and $\varepsilon'' = C''C_0^{-1}$, with a vacant capacitance (C_0).

The sample film for dielectric relaxation measurement was prepared as follows. Bulk $PC_2VITFSI$ polymer was molded by use of a hot press at 120 °C to make a plane film. The resulting $PC_2VITFSI$ film was transparent with a slight orange tinge and had a film thickness of 86 μm. Next, Au was vacuum deposited onto both faces of the film to serve as electrodes. The sample film was then mounted inside the homemade sample cell, in which the temperature was controlled by the combination of a heater (DSSP23, Shimaden, Tokyo, Japan) and a chiller (UT-2000, EYELA, Tokyo, Japan). The measurement temperature ranged from −90 to +90 °C.

Results

Differential Scanning Calorimetry. Figure 2 shows the DSC profiles of bulk $PC_2VITFSI$ sample. The upper and lower curves represent the total heat flow during the cooling and heating processes, respectively. Thermal transitions were observed at 56 °C on both the cooling and heating curves. A weak thermal transition was observed in the heating curve at −72 °C.

In Ohno's early study, the T_g of $PC_2VITFSI$ was reported as −75.4 °C.[8] On the other hand, Vygodskii reported that $PC_2VITFSI$ exhibited a glass transition at 60 °C.[11] Both T_g values reported by Onho and Vygodskii are respectively similar to the temperatures of −72 and 56 °C, at which thermal transitions are observed in our DSC measurement. In our experimental observation, bulk $PC_2VITFSI$ seemed to become soft for temperatures over 100 °C, and they were successfully molded to make films using a hot press technique at 120 °C. Therefore, we conclude that the T_g of $PC_2VITFSI$ is 56 °C. The origin of the thermal transition observed at −72 °C would concern with local motions of $PC_2VITFSI$. However, we cannot further discuss the transition from our DSC and DR data.

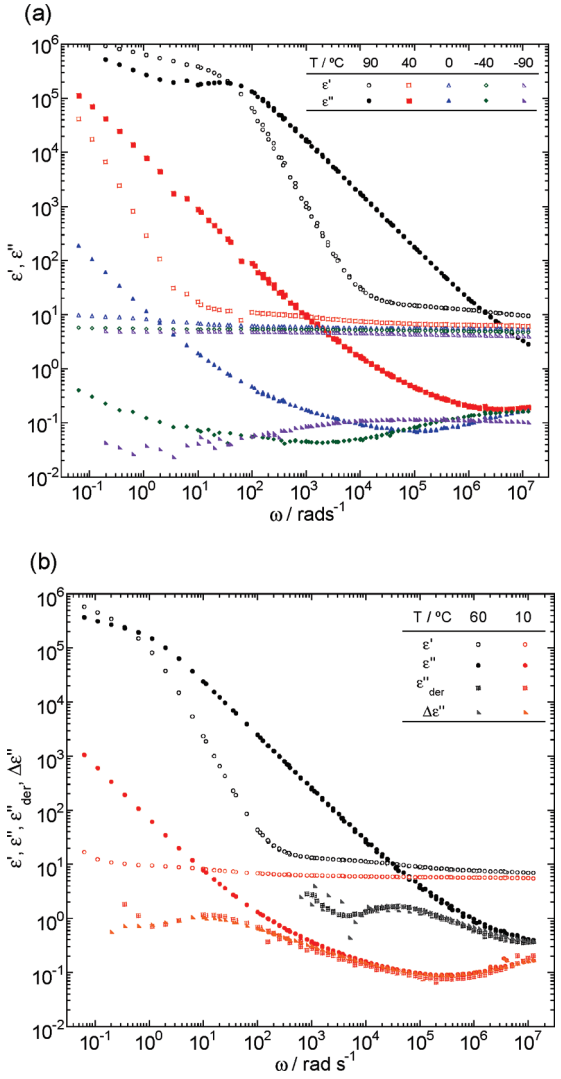

Figure 3. (a) Dependence of the real and imaginary parts of electric permittivities, ε' and ε'', on angular frequency, ω, for $PC_2VITFSI$ at various temperatures. (b) Dependence of ε' and ε'' on ω for $PC_2VITFSI$ at 60 and 10 °C. This figure also includes the dependence of the permittivities following elimination of the contributions of direct current conductivity, ε''_{der} and $\Delta\varepsilon''$, calculated using eqs 1 and 2, respectively, on ω for $PC_2VITFSI$ at 60 and 10 °C.

Dielectric Relaxation Behavior. Figure 3a shows DR spectra, ε' and ε'', as functions of angular frequency ω for $PC_2VITFSI$ at various temperatures. Three DR modes were observed in this system. First, the ε'' spectrum at −90 °C reveals a broad relaxation over 10^3 rad s^{-1}. This relaxation mode, labeled β, shifts to a higher frequency regime with increasing temperature, and finally moves out of the measurement frequency range at over 0 °C. Second, remarkably sharp increases in the ε' and ε'' curves were observed in the lower frequency regime at over 40 °C. This increase in the ε' and ε'' curves was due to the electrode polarization effect and the direct current conductivity of the sample, respectively. At 90 °C, clear DR with a magnitude of the relaxation strength of ca. 10^5 is observed due to the electrode polarization behavior. We label this relaxation mode EP. Third, the ε' spectrum at 40 °C reveals a rather broad relaxation, labeled α, in the frequency regime $10^2 < \omega < 10^5$ rad s^{-1}. The effect of direct current conductivity was so strong that it masks α relaxation mode in the ε'' spectrum.

In order to eliminate the contribution of the direct current conductivity from the ε'' spectrum, we employed the following derivative relationship.

$$\varepsilon''_{der} = -\frac{\pi}{2}\frac{\partial\varepsilon'(\omega)}{\partial[\ln\omega]} \quad (1)$$

This provides an approximately conduction-free ε'' spectrum in the frequency range where ε' contains no electrode polarization effects.[32,33] Figure 3(b) shows the dependence of ε', ε'' and ε''_{der} on ω for $PC_2VITFSI$ at 60 and 10 °C. ε'' continued to rise with a decrease in ω due to the strong contribution of direct current conductivity. However, ε''_{der} spectra showed a peak in the frequency region, where the α relaxation mode is observed in terms of the ε' spectrum. In order to confirm the validity of ε''_{der}, we also evaluated another conduction-free ε'', $\Delta\varepsilon''$, by subtracting the contribution of the direct current conductivity from ε'' as

$$\Delta\varepsilon'' = \varepsilon'' - \frac{\kappa}{\omega\varepsilon_0} \quad (2)$$

where ε_0 is the permittivity of a vacuum and κ is the specific direct current conductivity evaluated from the plateau value of $\kappa(\omega) = C''\omega\varepsilon_0 C_0^{-1}$. Figure 3b also shows the relationship between $\Delta\varepsilon''$ and ω for $PC_2VITFSI$. The correspondence between ε''_{der} and $\Delta\varepsilon''$ strongly supports the validity of regarding ε''_{der} as the conduction-free ε'' spectrum and the presence of a α relaxation mode. Essentially the same behavior between ε''_{der} and $\Delta\varepsilon''$ was observed at all the measurement temperatures. The ε'' and ε''_{der} spectrum are similar at temperatures of less than −40 °C, at which the contribution of the direct current conductivity is weakened significantly. In the following discussion, we used ε'' as the dielectric loss spectra to fit the total relaxation modes including α, β and EP and use ε''_{der} as the loss spectra to fit the sum of α and β relaxation modes.

Master curves of ε'' and ε''_{der} for $PC_2VITFSI$ are shown in parts a and b of Figure 4, respectively. Dielectric loss curves at any given temperature are superimposed on data at a reference temperature T_0, using a frequency scale multiplicative shift factor a_T and a permittivity scale multiplicative shift factor b_T. Figure 4a, in which T_0 is set at −90 °C, focuses on the β relaxation mode. It seemed that $b_T\varepsilon''$ spectra were well superimposed each other in the frequency range of $a_T\omega >$ 10 rad s^{-1} where β relaxation mode is present. Alternately, the ε'' spectra failed to superimpose in the frequency range of $a_T\omega <$ 10 rad s^{-1}. We fit the master curve around the β relaxation mode by assuming a simple relaxation mode, which was expressed as the imaginary part of Havriliak−Negami type relaxation formula as

$$\Delta\varepsilon^* = \frac{\Delta\varepsilon}{(1+(ia_T\omega\tau)^p)^q} \quad (3)$$

where $\Delta\varepsilon$ and τ are the relaxation strength and time constant, respectively, and p and q represent the broadening factors of spectrum. Figure 4a also shows the best fit curve of the β relaxation mode using eq 3 with parameters of $\Delta\varepsilon = 2.00$, $\tau = 0.80$ ms, $p = 0.35$, and $q = 0.17$.

We set T_0 at 50 °C for the ε''_{der} master curve shown in Figure 4b to focus on the α relaxation mode. $b_T\varepsilon''_{der}$ spectra superimpose well over each other in the frequency range of $a_T\omega < 10^6$ rad s^{-1}, however they deviate from each other in the frequency range of $a_T\omega > 10^6$ rad s^{-1} due to the overlap of the β relaxation mode. We fit the α relaxation mode in the same manner as the β relaxation mode. Figure 4b also includes the best fit curve of the α relaxation mode using

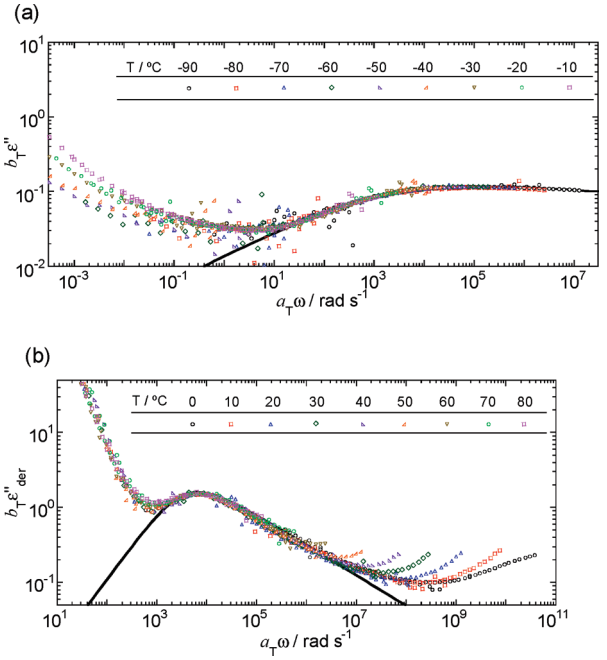

Figure 4. Master curves of: (a) ε'' with the reference temperature, T_0, set at −90 °C and (b) ε''_{der} with T_0 set at 50 °C for $PC_2VITFSI$. a_T and b_T mean the frequency and permittivity scale multiplicative shift factor, respectively. Solid lines represent the best fit curves for (a) $b_T\varepsilon''$ and (b) $b_T\varepsilon''_{der}$ calculated using eq 3.

eq 3 with parameters of $\Delta\varepsilon = 5.50$, $\tau = 0.32$ ms, $p = 0.90$, and $q = 0.45$.

The poor agreement of the dielectric loss curves with the data over some frequency regions in both parts a and b of Figure 4 indicates that the temperature dependence of the α relaxation mode is different from that of the β relaxation mode. However, the agreement of the loss spectra around each relaxation mode indicates that the broadening factors p and q contained in eq 3 are less dependent on the temperature.

As mentioned above, the α and β relaxation modes are well described by the Havriliak−Negami formula represented in eq 3. It has been found that the DR mode attributed to the electrode polarization behavior is well described using modified Macdonald's theory.[34,35] Macdonald's theory is a classic theory regarding the electrode polarization effect in materials containing conductive ionic species. According to Macdonald's theory, DR spectra due to the electrode polarization effect are essentially described with a modified Debye type relaxation function:

$$\varepsilon_{EP}^* = \frac{\varepsilon_{EP}}{(i\omega\tau_{EP})^{1-n} + i\omega\tau_{EP}} \qquad (4)$$

where τ_{EP} and ε_{EP} is the relaxation time and strength due to the electrode polarization and the exponent n ($0 < n \leq 1$) reflects the electrode roughness.[36,37] It is important to note that further analyses of τ_{EP} and ε_{EP} in eq 4 using Macdonald's theory provide the mobility and the free ion concentration of an ionic species in the system.[34] However this estimation is only valid when there is one type charge carrier and low ion contents in the system.[29] Since $PC_2VITFSI$ system is concentrated ionic system, the estimation of the mobility and the free ion concentration of $TFSI^-$ using Macdonald's theory must fail. Consequently, we use eq 4 to describe the relaxation spectra due to electrode polarization relaxation mode and estimate the τ_{EP} and ε_{EP} in this study.

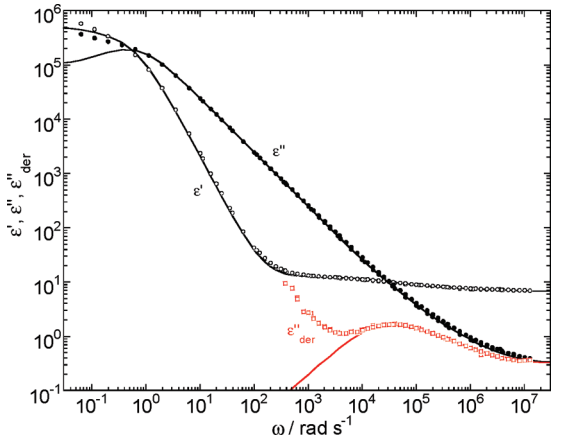

Figure 5. Dependence of ε', ε'', and ε''_{der} on ω for $PC_2VITSFI$ at 60 °C. Black solid lines indicate the best fit curves for ε' and ε'' calculated by eq 5 and red solid line indicates the best fit curve for ε''_{der} calculated using eq 5 without the ε_{EP}* term.

DR spectra, ε' and ε'', of $PC_2VITFSI$ system were well described as the summation of two Havriliak−Negami type relaxation formulas and a relaxation mode predicted by a modified Macdonald's theory as follows.

$$\varepsilon^* = \varepsilon_{EP}^* + \varepsilon_\alpha^* + \varepsilon_\beta^* + \varepsilon_\infty = \frac{\varepsilon_{EP}}{(i\omega\tau_{EP})^{1-n} + i\omega\tau_{EP}} + \frac{\varepsilon_\alpha}{(1+(i\omega\tau_\alpha)^{p_\alpha})^{q_\alpha}} + + \frac{\varepsilon_\beta}{(1+(i\omega\tau_\beta)^{p_\beta})^{q_\beta}} + \varepsilon_\infty \qquad (5)$$

Here ε_i and τ_i are the dielectric relaxation strength and time for each relaxation mode i, respectively, and p_i, q_i are the broadening factors for the spectrum of each relaxation mode i. ε_∞ is the high frequency limiting permittivity observed in the ε' spectra. We also reproduced ε''_{der} spectra using eq 5 with the treatment of subtracting the first ε_{EP}* term.

Since the shape of the ε'' and ε''_{der} master curves are less dependent on the measurement temperature (Figure 4, parts a and b), we fixed a portion of the variable parameters concerning the broadening factor in eq 5 as $p_\alpha = 0.90$, $p_\beta = 0.35$, and $n = 0.90$. We also attempted to describe the DR spectra by varying ε_∞, ε_i, and τ_i of each relaxation mode and the broadening factors q_α, q_β. Figure 5 shows a typical example of the best fit curves for ε', ε'', and ε''_{der} spectra with parameters $\varepsilon_\infty (+ \varepsilon_\beta) = 6.93$, $\varepsilon_{EP} = 3.60 \times 10^5$, $\tau_{EP} = 1.4$ s, $\varepsilon_\alpha = 5.20$, $\tau_\alpha = 60$ μs, $p_\alpha = 0.90$, and $q_\alpha = 0.48$ for $PC_2VITFSI$ at 60 °C. The fitting curve is represented by a red solid line and describes the ε''_{der} spectrum around the α relaxation mode well. The fitting curves represented by the black solid lines also describes the ε' and ε'' spectra well, except in the frequency regime where $\omega < 10$ rad s^{-1}; in this region the effect of electrode polarization is dominant. Since the volume of bis(trifluoromethanesulfonylimide) ($TFSI^-$) ions are much smaller than that of poly(1-ethyl-3-vinylimidazolium) (PC_2VI^+) polyions, the DR mode observed around $\omega = 10$ rad s^{-1} is attributed to the electrode polarization behavior due to the translational diffusion of $TFSI^-$ ions. Thus, the deviation between fitting curves and DR spectra observed at $\omega < 10$ rad s^{-1} implies the presence of another relaxation mode, probably attributable to an electrode polarization effect due to the diffusion of PC_2VI^+ polyions, in the lower part of the frequency regime. Other DR spectra at any given temperature were also described well by eq 5 with the broadening parameters q_α ranging from 0.37 to 0.45 and q_β between 0.17 and 0.75.

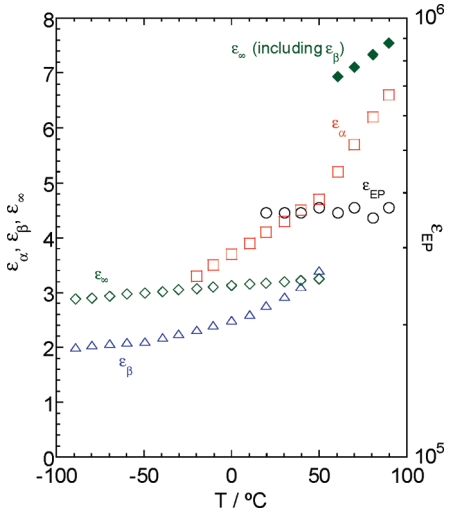

Figure 6. Dependence of the relaxation strength, ε_{EP}, ε_α, and ε_β, for each relaxation mode and high frequency limiting permittivity, ε_∞, on temperature, T, for $PC_2VITFSI$. At temperatures higher than 60 °C, ε_∞ (filled symbols) includes the contribution of ε_β because the β relaxation mode was not observed in the measurement frequency regime at these temperatures.

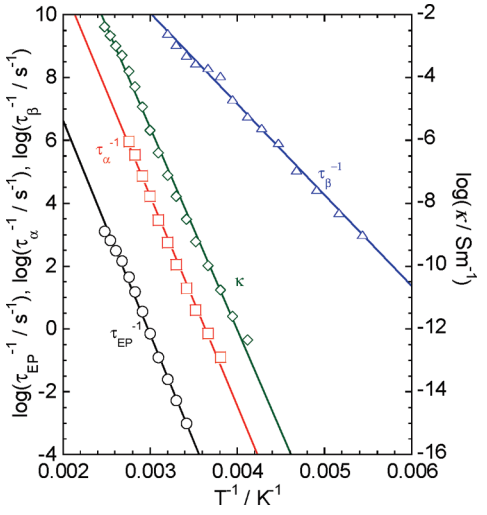

Figure 7. Arrhenius plot of reciprocal of relaxation time, τ_{EP}, τ_α, and τ_β, and specific direct current conductivity, κ, for $PC_2VITFSI$.

Figure 6 shows the temperature dependence of dielectric parameters, ε_i and ε_∞, obtained from the fitting procedure for $PC_2VITFSI$. Since the β relaxation mode is present in a higher frequency region than our measurement frequency range at over 60 °C, the values of ε_∞ mean the sum of ε_∞ and ε_β at their temperature (shown as filled symbol in Figure 6). ε_α, ε_β, and ε_∞ increase with increasing temperature but ε_{EP} seems constant with respect to temperature. The relationship between fitting parameters of τ_i for each relaxation mode i and temperature is summarized in Figure 7 as an Arrhenius plot profile. Figure 7 also includes an Arrhenius Plot of the specific direct current conductivity, κ, for $PC_2VITFSI$. All τ_i and κ show an Arrhenius-type temperature dependence, which can be represented as

$$\tau_i^{-1} \quad \text{or} \quad \kappa \propto \exp\left(-\frac{E}{kT}\right) \tag{6}$$

where k is the Boltzmann coefficient and E is the activation energy. The values of E for all the relaxation modes are summarized in Table 1.

Table 1. Activation Energy, E, Obtained from the Arrhenius Plot (Figure 7) of Reciprocal Relaxation Times, τ_{EP}, τ_α, and τ_β, for each Relaxation Mode and Specific Direct Current Conductivity, κ, Calculated Using eq 6 for $PC_2VITFSI$

	E/kJ mol^{-1}
EP	129
α	119
β	56
κ	123

Discussion

Glass Transition Dynamics. It has been known that certain DR modes, like segmental motion observed in polymer systems, exhibit Vogel−Fulcher−Tamman (VFT) temperature dependence. This dependence can be represented by

$$\tau_i^{-1} \quad \text{or} \quad \kappa \propto \exp\left(\frac{U}{T - T_0}\right) \tag{7}$$

where U is the activation temperature and T_0 is the Vogel temperature at which τ_i or κ goes to infinity or zero, respectively. Thus, T_0 generally correlates to T_g and is typically about 50 K below T_g. In ionomer systems, relaxation modes due to segmental motion and motion of the ion-pairs formed between a charge unit in a polymer chain and a counterion are observed.[28,29] The relaxation times of these relaxation modes and κ of the ionomer system exhibit VFT temperature dependence.[27−29,38] In an IL system with a glass transition temperature, DR times due to the electrode polarization behavior and κ also show the VFT temperature dependence.[39,40]

Figure 6 shows the crucial findings that temperature dependences of all τ_i and κ are unable to be reproduced by the VFT equation (eq 7). If certain relaxation modes or conductivity in a $PC_2VITFSI$ system are VFT temperature dependent, then their relaxation times or κ should converge to the asymptotic value of 0.0036 K^{-1} ($=(T_g - 50)^{-1}$). A similar, less fragile relationship between temperature and conductivity were observed in other PIL systems.[15] Elabd et al. investigated the conductivity of some PILs, poly(1-[(2-methacryloxy)ethyl]-3-butylimidazolium tetrafluoroborate) (T_g = 71.5 °C) or poly(1-[(2-methacryloxy)ethyl]-3-butylimidazolium bis(trifluoromethanesulfonyl)imide) (T_g = −15 °C) and others.[15] The temperature dependence of their conductivity were well reproduced using either Arrhenius or VFT equations.

Consequently, we believe that the less fragile behavior is an essential property for PILs. One might suppose that how PILs transport $TFSI^-$ ions below T_g contrasts with such fragile materials as ionomers and ILs. We have included a speculative interpretation of the $TFSI^-$ transport mechanism for $PC_2VITFSI$ in Figure 8. Bulk $PC_2VITFSI$ is filled by charged 1-ethyl-3-vinylimidazolium (C_2VI^+) units on polymer chains and $TFSI^-$ ions, and the distance between plural C_2VI^+ units is closer than the distance between charged units in an ionomer system. Therefore, a $TFSI^-$ ion forming an ion-pair with a charged C_2VI^+ unit may change its interaction partner to another C_2VI^+ unit neighboring the $TFSI^-$ ion. This process is associated with the rotation of side chains including the ion-pair around the main chain (side chains are able to move below T_g). $TFSI^-$ ions would be transported upon repetition of the ion-pair formation and dissociation processes, therefore $PC_2VITFSI$ will be conductive at temperatures below T_g.

Assignment of Relaxation Modes. The $PC_2VITFSI$ system exhibited three relaxation modes, α, β, and EP. We conclude that the EP relaxation mode is attributed to electrode polarization behavior because the magnitude of the dielectric

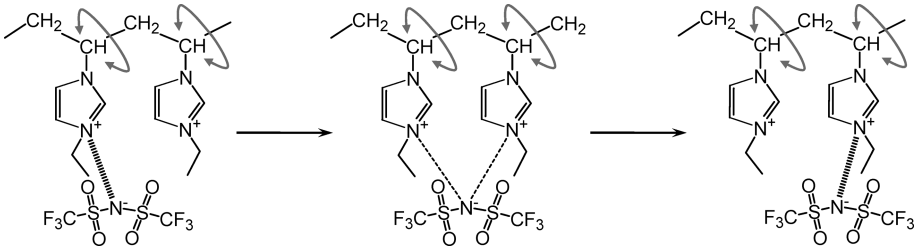

Figure 8. Schematic representation of the proposed anion transport mechanism for $PC_2VITFSI$. This mechanism is associated with the rotation of side chain on the axis of the $PC_2VITFSI$ main chain and the formation and dissociation of ion-pairs formed between $TFSI^-$ and a charge unit of PC_2VI^+.

strength is the order of 10^5. In this section, we attempted to assign α and β relaxation modes.

We first survey what relaxation modes would be observed in PIL system. Ionomer system shows relaxation modes attributable to segmental motion of polymer chain and ion-pair motion formed between a electrolyte monomer unit and a counterion.[28,29] According to the dielectric studies of ionomer system studied by Runt et al., ion-pair relaxation mode appears at a frequency lower than that of polymer segmental relaxation mode.[29] The DR mode attributed to the ion-pair dynamics is also observed in aqueous dilute polyelectrolyte solution.[41] Therefore, reorientation dynamics of ion-pairs would be the common DR mode in the polyelectrolyte system. In an IL system, DR modes due to the rotational motions of the polarized anions and cations are observed when anions or cations in IL molecules have asymmetric chemical structures. For example, 1-ethyl-3-methylimidaozlium bis(trifluoromethanesulfonylimide), whose chemical structure is similar to that of the $PC_2VITFSI$ monomer unit, shows DR modes due to the rotational motion of the 1-ethyl-3-methylimidaozlium in the GHz frequency region.[22,24] This fact indicates that the DR mode due to the rotational motion of C_2VI^+ side chain on the axis of polymer backbone would be observed in the $PC_2VITFSI$ system. Accordingly, we regard the following molecular motions, in the order of slow dynamics, as the candidates for the DR mode of $PC_2VITFSI$ (Figure 9): ion-pair, segmental motion, rotational motion of C_2VI^+ side chains and rotational motion of $TFSI^-$ anions.

The magnitude of the relaxation strength of the α relaxation mode (3.5−6.6) in $PC_2VITFSI$ is similar to that of the segmental relaxation motion (2−7) but is very different from that of the ion-pair relaxation mode (20−120) observed in ionomer systems.[28,29] It has been shown that the relaxation strength due to the ion-pair relaxation mode increases with an increasing number of electrolyte units on the polymer chain.[29,41] If the α relaxation mode in $PC_2VITFSI$ derives from the ion-pair relaxation mode, then the relaxation strength of α relaxation mode must be higher than that of the ionomer systems; because the number of electrolyte units per unit volume in the $PC_2VITFSI$ system is much higher than that of the ionomer systems. The fact that the magnitude of the relaxation strength of α relaxation mode in $PC_2VITFSI$ is lower than that of the ion-pair relaxation mode in an ionomer system strongly suggests that the α relaxation mode in $PC_2VITFSI$ should be attributed to polymer segmental motion (Figure 9). We emphasize again that PIL system has a less fragile property, thus it seems reasonable to attribute the α relaxation mode to either an ion-pair or segmental relaxation mode, though these relaxation modes exhibit VFT temperature dependence in an ordinary polymer or ionomer system.

The results of the Arrhenius plot in Figure 6 provide another possibility for the attribution of the α relaxation

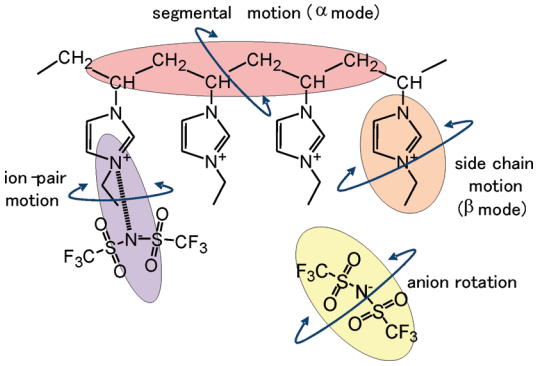

Figure 9. Schematic representation of the candidates for relaxation modes observed in $PC_2VITFSI$.

mode. The value of E for the EP relaxation mode is similar to that of κ, ca. 120 kJ mol^{-1} (Table 1). This finding is reasonable because the EP relaxation mode and direct current conductivity derive from the same phenomenon, i.e. translational diffusion of mobile ions. However, the value of E for the α relaxation mode is also similar to those for EP relaxation mode and κ. This finding implies that the origin of the α relaxation mode may be electrostatic interaction or charge transport behavior; these are the origin of the EP relaxation mode or direct current conductivity. In other words, this finding provides the possibility that the α relaxation mode may derive from ion-pair motion rather than polymer segmental motion. Since Runt et al. suggested that ion-pair motion over the scale of a few angstroms must involves the several rearrangements of the neighboring polymer segments in the ionomer system,[29] it seems natural that the value of E for the segmental relaxation mode is similar to that of the ion-pair relaxation mode in bulk polyelectrolyte systems such as ionomers and PILs.

One might wonder at the absence of an ion-pair relaxation mode in $PC_2VITFSI$ system. According to the ionomer study by Runt et al.,[29] an ion-pair relaxation mode occurs in the ionomers at frequencies approximately 2 orders of magnitude lower than that of the polymer segmental relaxation mode. Figure 5 shows that the effect of the electrode polarization is dominant around the frequency of 4.0×10^2 rad s^{-1}, which is the 2 orders of magnitude lower than the peak frequency of α relaxation mode (4.0×10^4 rad s^{-1}), at 60 °C. Therefore, we cannot further discuss the presence of an ion-pair relaxation mode in the $PC_2VITFSI$ system if its relaxation mode appears around the frequency regime from 10^2 to 10^3 rad s^{-1}. If the $TFSI^-$ transport mechanism associated with ion-pair reorientation actually occurs as schematically represented in Figure 8, then the DR mode due to rotational motion of ion-pair should be present.

The 56 kJ mol^{-1} value of E for the β relaxation mode was lower than those for the κ, α and EP relaxation mode,

ca. 120 kJ mol^{-1} (Table 1). This indicates that the origin of the β relaxation mode differs from those of α and EP relaxation modes. The molecular dynamics attributed to the β relaxation mode is faster than that attributed to the α relaxation mode, i.e. segmental relaxation mode. Therefore, the β relaxation mode should be assigned to the rotational relaxation motion of C_2VI^+ side chains attached to the polymer main chain, or to the rotational motion of $TFSI^-$ ion in the bulk. In our experimental frequency and temperature range, only one relaxation mode (β relaxation mode) is observed. The relaxation mode due to the side chain motion must be slower than that attributed to the rotational relaxation mode of the $TFSI^-$ ion, consequently we assign the β relaxation mode to the rotational relaxation motion of polymer side chain (Figure 9). The DR mode due to the rotational relaxation of $TFSI^-$ would be present in a higher frequency range than the measurement frequency regime used in this study.

Conclusion

We investigated the dielectric relaxation behavior of polymerized ionic liquid, poly(1-ethyl-3-vinylimidazolium bis(trifluoromethanesulfonylimide)) ($PC_2VITFSI$) over a wide frequency, 10 mHz to 2 MHz, and temperature range, −90 to +90 °C. Three relaxation modes including that of electrode polarization were observed. Relaxation times of these relaxation modes and the specific direct current conductivity showed an Arrhenius-type temperature dependence. This was so even if they crossed the temperature corresponding to the glass transition temperature of $PC_2VITFSI$, 56 °C. We believe that less fragile behavior is the essential property for the polymerized ionic liquids and suppose that the charge transport mechanism is achieved by an anion relay process, even at temperatures below the glass transition temperature; this is facilitated by the interaction between one and another ion-pair through the rotational motion of side chains on the axis of the polymer main chain. The slower relaxation mode is assigned to the segmental relaxation mode of the polymer because the magnitude of its dielectric strength is similar to that of segmental relaxation mode observed in an ionomer system. The faster relaxation mode is attributed to the rotational relaxation mode of the polymer side chain. DR modes due to an ion-pair relaxation mode and rotational relaxation motion of $TFSI^-$ in the bulk polymer should be observed in this system; however, these relaxation modes were absent in the experimental data obtained from the frequency and temperature regime used in this study.

Acknowledgment. This work was supported by a Grant-in-Aid for Young Scientists (B) (No. 21750131) from the Japan Society for the promotion of Science. This work was also supported by Grant-in-Aid for Scientific Research on Priority Area "Soft Matter Physics" from the Ministry of Education, Culture, Sports, Science and Technology of Japan.

Supporting Information Available: Figure S1 showing the ^{1}H NMR spectra for synthesized $C_2VITFSI$ and $PC_2VITFSI$. This material is available free of charge via the Internet at http://pubs.acs.org.

References and Notes

(1) Wilkes, J. S.; Zaworotko, M. *J. Chem. Soc., Chem. Commun.* **1992**, 965.
(2) Welton, T. *Chem. Rev.* **1999**, *99*, 2071.
(3) Wasserscheid, P.; Welton, T., *Ionic Liquids in Synthesis*; Wiley-VCH: Weinheim, Germany, 2003.
(4) Dupont, J.; de Souza, R. F.; Suarez, P. A. Z. *Chem. Rev.* **2002**, *102*, 3667.
(5) Galiński, M.; Lawandowski, A.; Stępaniak, I. *Electrochim. Acta* **2006**, *51*, 5567.
(6) Dupont, J.; Suarezb, P. A. Z. *Phys. Chem. Chem. Phys.* **2006**, *8*, 2441.
(7) Matsumoto, K.; Hagiwara, R. *J. Fluorine Chem.* **2007**, *128*, 317 and references therein.
(8) Ohno, H.; Ito, K. *Chem. Lett.* **1998**, 751.
(9) Tang, J.; Tang, H.; Sun, W.; Plancher, H.; Radosz, M.; Shen, Y. *Chem. Commun.* **2005**, 3325.
(10) Nakashima, T.; Kawai, T. *Chem. Commun.* **2005**, 1643.
(11) Ohno, H. *Bull. Chem. Soc. Jpn.* **2006**, *79*, 1665 and references therein.
(12) Marcilla, R.; Blazquez, J. A.; Fernandez, R.; Grande, H.; Pomposp, J. A.; Mecerreyes, D. *Macromol. Chem. Phys.* **2005**, *206*, 299.
(13) Vygodskii, Y. S.; Mel'nik, O. A.; Lozinskaya, E. I.; Shaplov, A. S.; Malyshkina, I. A.; Gavrilova, N. D.; Lyssenko, K. A.; Antipin, M. Y.; Golovanov, D. G.; Korlyukov, A. A.; Ignat'ev, N.; Welz-Biermann, U. *Polym. Adv. Technol.* **2007**, *18*, 50.
(14) Chen, H.; Elabd, Y. A. *Macromolecules* **2009**, *42*, 3368.
(15) Chen, H.; Choi, J.; Salas-de la Cruz, D.; Winey, K. I.; Elabd, Y. A. *Macromolecules* **2009**, *42*, 4809.
(16) Hara, M., Ed. *Polyelectrolytes: Science and Technologies*; Marcel Dekker: New York, 1992.
(17) Dobrynin, A. V.; Rubinstein, M. *Prog. Polym. Sci.* **2005**, *30*, 1049.
(18) Marcilla, R.; Blazquez, A.; Rodriguez, J.; Pomposo, J. A.; Mecerreyes, D. *J. Polym. Sci., Part A* **2004**, *42*, 208.
(19) Kremer, F., Schohals, A., Eds. *Broadband Dielectric Spectroscopy*; Springer-Verlag: Berlin, 2002.
(20) Runt, J., Fitzgerald, J. J., Eds. *Dielectric Spectroscopy of Polymeric Materials: Fundamentals and Applications*; American Chemical Society: Washington, DC, 1997.
(21) Barsoukov, E., Macdonald, J. R., Eds. *Impedance Spectroscopy: Theory, Experiment, and Applications*, 2nd ed.; Wiley: New York, 2005.
(22) Daguenet, C.; Dyson, P. J.; Krossing, I.; Oleinikova, A.; Slattery, J.; Wakai, C.; Weingärtner, H. *J. Phys. Chem. B* **2006**, *110*, 12682.
(23) Stoppa, A.; Hunger, J.; Buchner, R.; Hefter, G.; Thomas, A.; Helm, H. *J. Phys. Chem. B* **2008**, *112*, 4854.
(24) Nakamura, K.; Shikata, T. *ChemPhysChem* **2010**, *11*, 285.
(25) Tang, J.; Radosz, M.; Shen, Y. *Macromolecules* **2008**, *41*, 493.
(26) Ogihara, W.; Washiro, S.; Nakajima, H.; Ohno, H. *Electrochim. Acta* **2006**, *51*, 2614.
(27) Klein, R. J.; Zhang, S.; Dou, S.; Jones, B. H.; Colby, R. H.; Runt, J. *J. Chem. Phys.* **2006**, *124*, 144903.
(28) Fragiadakis, D.; Dou, S.; Colby, R. H.; Runt, J. *Macromolecules* **2008**, *41*, 5723.
(29) Fragiadakis, D.; Dou, S.; Colby, R. H.; Runt, J. *J. Chem. Phys.* **2009**, *130*, 064907.
(30) Oyama, T.; Kawahara, K.; Ueda, M. *Nippon Kagaku Zasshi* **1958**, *79*, 727.
(31) Brandrup, J.; Immergut, E. H.; Grulke, E. A. *Polymer HandBook*, 4th ed; Wiley: New York, 1999.
(32) Steeman, P. A. M.; van Turnhout, J. *Macromolecules* **1994**, *27*, 5421.
(33) Wübbenhorst, M.; van Turnhout, J. *J. Non-Cryst. Solids* **2002**, *305*, 40.
(34) Macdonald, J. R. *Phys. Rev.* **1953**, *92*, 4.
(35) Coelho, R. J. *J. Non-Cryst. Solids* **1991**, *131*, 1136.
(36) Bordi, F.; Cametti, C.; Colby, R. H. *J. Phys.: Condens. Matter* **2004**, *16*, R1432.
(37) Pajkossy, T. *Solid State Ionics* **2005**, *176*, 1997.
(38) Kline, R. J.; Welna, D. T.; Weikel, A. L.; Allcock, H. R.; Runt, J. *Macromolecules* **2007**, *40*, 3990.
(39) Tokuda, H.; Hayamizu, K.; Ishii, K.; Susan, M. A. B. H.; Watanabe, M. *J. Chem. Phys. B* **2005**, *109*, 6103.
(40) Sangoro, J. R.; Serghei, A.; Naumov, S.; Galvosas, P.; Kärger, J.; Wespe, C.; Bordusa, F.; Kremer, F. *Phys. Rev. E* **2008**, *77*, 051202.
(41) Nakamura, K.; Shikata, T. *Macromolecules* **2006**, *39*, 1577.